

Investigation of Signals and Transcription Factors for The Generation of Female Germ-Like Cells

Saman Ebrahimi, Ph.D.¹, Alireza Shams, Ph.D.^{2*}, Parvaneh Maghami, Ph.D.¹, Azadeh Hekmat, Ph.D.¹

1. Department of Biology, Science and Research Branch, Islamic Azad University, Tehran, Iran
2. Department of Anatomy, School of Medicine, Alborz University of Medical Sciences, Karaj, Iran

*Corresponding Address: P.O.Box: 3149969415, Department of Anatomy, School of Medicine, Alborz University of Medical Sciences, Karaj, Iran
Email: dr.shams@abzums.ac.ir

Received: 11/October/2021, Accepted: 27/February/2022

Abstract

Objective: Primordial germ cell (PGCs) lines are a source of a highly specialized type of cells, characteristically oocytes, during female germline development *in vivo*. The oocyte growth begins in the transition from the primary follicle. It is associated with dynamic changes in gene expression, but the gene-regulating signals and transcription factors that control oocyte growth remain unknown. We aim to investigate the differentiation potential of mouse bone marrow mesenchymal stem cells (mMSCs) into female germ-like cells by testing several signals and transcription factors.

Materials and Methods: In this experimental study, mMSCs were extracted from mice femur bone using the flushing technique. The cluster-differentiation (CD) of superficial mesenchymal markers was determined with flow cytometric analysis. We applied a set of transcription factors including retinoic acid (RA), titanium nanotubes (TNTs), and fibrin such as TNT-coated fibrin (F+TNT) formation and (RA+F+TNT) induction, and investigated the changes in gene, *MVH/DDX4*, expression and functional screening using an *in vitro* mouse oocyte development condition. Germ cell markers expression, (*MVH / DDX4*), was analyzed with Immunocytochemistry staining, quantitative transcription-polymerase chain reaction (RT-qPCR) analysis, and Western blots.

Results: The expression of CD was confirmed by flow cytometry. The phase determination of the TNTs and F+TNT were confirmed using x-ray diffraction (XRD) and scanning electron microscope (SEM), respectively. Remarkably, applying these transcription factors quickly induced pluripotent stem cells into oocyte-like cells that were sufficient to generate female germ-like cells, growth, and maturation from mMSCs differentiation. These transcription factors formed oocyte-like cells specification of stem cells, epigenetic reprogramming, or meiosis and indicate that oocyte meiosis initiation and oocyte growth are not separable from the previous epigenetic reprogramming in stem cells *in vitro*.

Conclusion: Results suggested several transcription factors may apply for arranging oocyte-like cell growth and supplies an alternative source of *in vitro* maturation (IVM).

Keywords: Cell Differentiation, Germ cells, Transcription Factors

Cell Journal (Yakhteh), Vol 24, No 8, August 2022, Pages: 458-464

Citation: Ebrahimi S, Shams A, Maghami P, Hekmat A. Investigation of signals and transcription factors for the generation of female germ-like cells. Cell J. 2022; 24(8): 458-464. doi: 10.22074/cellj.2022.8303.

This open-access article has been published under the terms of the Creative Commons Attribution Non-Commercial 3.0 (CC BY-NC 3.0).

Introduction

All infertile couples generate at least one meiotically incomplete oocyte, approximately 7 to 16% (1, 2). Oocyte maturation failure, a bad egg syndrome, is occasionally absolute means no mature oocytes are generated. The key clinical features associated with this syndrome include: i. Primary infertility, ii. Repetitive generation of mostly immature oocytes, iii. Inability of *in vitro* maturation (IVM) to stimulate maturation, and iv. Breakdown of fertilization despite intracytoplasmic sperm injection (ICSI) (3).

In oocyte differentiation, oocyte growth and meiosis are two key processes. Meiosis initiation is believed to be regulated mainly by retinol's production, storage, and metabolism and its metabolite retinoic acid (RA). RA signaling is performed by its target genes, such as *Stra8*, which is essential for the initiation and progression of meiosis. Intrinsic factors such as *MVH* provide diploid germ cells ready for meiosis initiation when extracellular signals are received (4).

Because of their characteristic properties, ability to

self-renewal, cloning, and differentiation into many different cell types as pluripotency, stem cells have been recommended in biomedical applications. Recently, much progress has been obtained in understanding stem cell biology and our ability to manipulate their proliferation and differentiation to get functional cells (5). Hübner et al. (6) show that mouse embryonic stem cells can develop into oogonia that enter meiosis; Bahmanpour et al. (7) improved the rate of *in vitro* oocyte differentiation by using bone morphogenetic protein 4 (BMP4) and RA along with ovarian somatic cell co-culture. Similarly, nanomaterials have recently been synthesized, which increases the efficiency of stem cell differentiation and their biomedicine applications, respectively (8, 9).

Growth and differentiation factors can adhere to nano-supplied surfaces and they can be effectively delivered into the culture medium. Therefore, functional scaffolds made of TNT can be used to grow, biocompatibility, differentiate stem cells, and regenerate damaged tissues (10). However, the small scale of nanomaterials alters their physicochemical properties, making their interactions

toxic to stem cells. Therefore, the determination of nanomaterial bio-interactions is essential to increase the success of medical treatments and enhance the safety of biomedical devices (11).

Fibrin, made from fibrinogen and thrombin, has been introduced as a suitable biological polymer in which tissue engineering applications and growth factors are delivered in cell cultures (12). Significant advantages of fibrin hydrogels include flexibility, low cytotoxicity, and high effectiveness on nanomaterials with homogeneous distribution (13). This characteristic leads to improved cell growth, viability, and differentiation in response to growth factors (14). According to the mentioned characteristics of fibrin, chemical, structural and mechanical, a 3D scaffold is suitable for later tissue engineering applications (15, 16).

Here, we applied a set of transcriptional factors, RA and RA+F+TNT formation, comprising the underlying gene regulatory expression and validated these findings with functional screening. Furthermore, we endeavored to reconstitute pluripotent stem cell differentiation and thereby we generated oocyte-like cells competent for oocyte meiosis initiation, oocyte growth, and subsequent fertilization *in vitro*.

Material and Methods

Nanoparticles synthesis

The TiO₂ nanoparticles were synthesized by the hydrothermal method described by Khoshnood et al. (17), then particles from 10 to 15 nm, which present micropores and mesopores on their surface, were obtained.

Isolation and culture

In this experimental study, the flushing technique was performed to isolate mouse bone marrow mesenchymal stem cells (mMSCs) from mice femur bone. The cell suspensions were transferred into 15 mL centrifugation tubes and were resuspended in DMEM medium (F12: REF:32500-035 Gibco, USA) supplemented with 10% FBS (Sigma-Aldrich, USA), 1% penicillin, and streptomycin (BI-1203 BIO IDEA Company, USA) mixture, and 1% Gluta MAX (Gibco, USA), and seeded in 25 cm² culture medium flask for maintaining at 37°C humidified incubator with 5% CO₂. At 80-90% confluency, cells were harvested with 0.05% Trypsin-EDTA solution (Gibco, USA) and replated in treatment groups (RA and RA+F+TNT formation). All protocols followed for the utilization of animals were approved by the Ethics Committee of Islamic Azad University, Science and Research Branch, Tehran, Iran, approval ID: IR.IAU.SRB.REC.1400.276.

Induction of stem cells into female germ-like cells

The cells obtained from the 3rd passage were used for signals and transcription factors to generate female germ-like cells. Then they were seeded at a density of 2×10⁴

per well in 24-well plates and treated with 10⁻⁵ M RA and 50 µg/ml TNT-coated fibrin (fibrinogen+thrombin 1:1) in the medium as mentioned above for 14 days. The Cells were observed for morphological changes during 14 days of induction, after which immunocytochemistry and quantitative transcription-polymerase chain reaction (RT-qPCR) were performed.

Morphology characterization of F+TNT formation

The phase characterization of TiO₂ nanoparticles was determined by X-ray diffraction pattern (XRD) (Model PW1730, PHILIPS, Cu LFF lamp λ=1.540598 Å, phase size=0.05°, phase time=1 second, voltage 40 kV, current 30 mA, And 40 mV). The 30λ TNT was then added by incubation at 50 µg/ml (18-20) of TNT-PBS-solution (21) on fibrin to measure their excess biological function and differential behavior. Figures analyzed with scanning electron microscope (SEM) and image j software (v. 1.52).

Flow cytometry analysis

For flow cytometric analysis of cluster-differentiation (CD) mesenchymal superficial markers, after four passages, 2×10⁴ cells were removed for a panel of mMSCs antibodies. The Cells were dispersed with 0.25%- trypsin-EDTA (Gibco, USA) and resuspended in PBS supplemented with 0.5% FBS. The cells were aliquoted into several parts and incubated at 4°C for 20 minutes in the dark with monoclonal antibodies (AB92574, AB114052, AB28364, and AB10558) against the hematopoietic cell markers CD31-PE and CD45-FITC (AB6785 and AB6717), and MSC markers CD90-PE, and CD105-FITC (AB6785 and AB6717). Negative control samples were incubated with mouse IgG1- FITC/PE (11-4724) isotype antibodies to help differentiate nonspecific background signals from specific antibody signals. The samples were analyzed on a Partec cytometer (German), and the resulting data were processed using FloMax software (22).

Immunocytochemistry

For Immunocytochemistry analysis of the specific germ cell marker, *MVH*, the cells were washed with PBS after 14 days of induction and were fixed in 4% paraformaldehyde for 20 minutes at 25°C. The cell membrane was permeabilized with 0.1% Triton X-100 solution in PBS for 20 minutes. Nonspecific binding-site blocking was performed with 5% goat serum for 45 minutes without washing, then incubation with anti-MVH (Mouse monoclonal anti-human, 1:100; Abcam, USA) antibody overnight at 4°C. Subsequently, the cells were washed with PBS and incubated with FITC-conjugated Goat Anti-Rabbit (1:100; Abcam, USA) or Goat Anti-Mouse (1:100; Abcam, USA) for 1 hour at 25°C. Finally, the Nuclei were counterstained with DAPI (Sigma, UK) for 5 minutes, and an Immunofluorescence image was taken using a fluorescent microscope (22).

Quantitative transcription-polymerase chain reaction

Using Tri-Pure reagent (Invitrogen, San Diego, CA, USA) whole RNA isolate per the manufacturer's instructions. The DNA contamination in the RNA sample was deleted by RNase-free DNase I (Thermo Scientific, USA) for 30 minutes at 37°C. The RNA concentration and purity were specified using the spectrophotometric (WPA spectrophotometer, Biochrom, UK) method. Using a Transcriptor First Strand cDNA Synthesis kit (Roche), the RNA was reversely transcribed by random Hexamer and 1000 ng of DNA-free RNA. TaqMan probe (Life Technologies, India) was applied to survey the expression of *MVH*, which normalized against 18 seconds expression as a housekeeping gene *β -actin*. The PCR reaction components were mixed to procure a final volume of 20 μ L. The following components were applied: 0.5 μ L (25 ng) cDNA, 1 μ L TaqMan assay reagent, 10 μ L TaqMan universal master mix, and 8.5 μ L distilled water. The PCR cycling was as follows: 10 minutes at 95°C, polymerase activation, 40 cycles at 95°C for 15 seconds, and 60°C for 1 minute using a Rotor-Gene Q instrument (Qiagen, Germany). The relative expression of the gene, using the $\Delta\Delta$ Ct method, was analyzed by normalizing the Ct values of the target against 18 seconds (22). Sequences of the *MVH* primers used for RT-qPCR are:

F: 5'GTGGAAGTGGTTCGAGGTGGT3'
R: 5'CTGGTGGAGGAGGGGTA3'

and primers sequences of housekeeping gene, *β -actin* are:

F: 5'TCAGAGCAAGAGAGGCATCC3'
R: 5'GGTCATCTTCTCACGGTTGG3'

Western blots

Fifty μ g of proteins extracted by RIPA lysis buffer was used for sodium dodecyl sulfate-polyacrylamide gel electrophoresis (SDS-PAGE) and transferred to nitrocellulose membranes. The membrane was stained with rabbit polyclonal antibody against MVH (AB13840, Abcam, UK, 1:100 dilutions), and goat anti-mouse secondary antibodies (ab6789, Lucerna-Chem, Switzerland). The antibody-antigen interaction in the membranes was observed using an enhanced-chemiluminescent detection kit (Santa Cruz Biotechnology Inc, Santa Cruz, CA, USA) (23).

Statistical analysis

All data were presented as mean \pm SD (standard deviation) and were analyzed using SPSS (v 23, IBM, USA). One-way ANOVA and Tukey tests followed by Bonferroni posttest were used to compare the groups. The significant differences ($P < 0.05$) were calculated among various treatment groups.

Results

Flow cytometry

We evaluated several stem cell-associated CD markers

using flow cytometry to determine the CD markers of cultured cells in passage 3. The results illustrate the differential characteristics of stem cells and rule out the hematopoietic origin of isolated cells. The Cells were mostly positive for mMSCs markers, CD90 and CD105, and at least reacted with hematopoietic markers, CD31 and CD45: 95% of the cells express CD90, 72.6% of the cells express CD105, 0.23% of the cells express CD31, and 1.42% of the cells express CD45 (Fig.1). Negative control samples were incubated with IgG1-FITC/PE isotype antibodies in mice. The data represented three independent experiments as mean \pm SD.

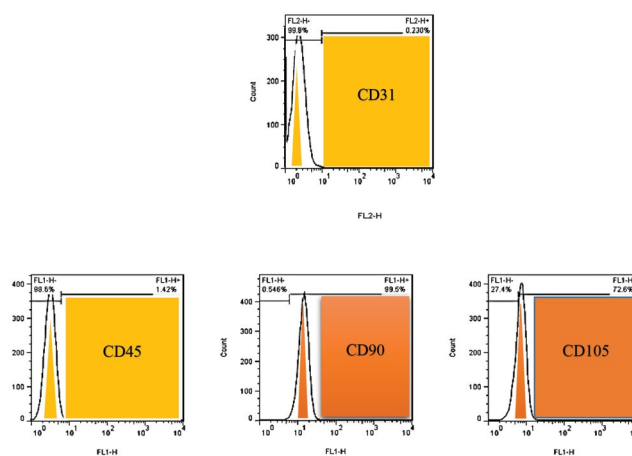


Fig.1: Flow cytometry results of CD expression in isolated mMSCs at third passage. The cells were mostly positive for the superficial mesenchymal markers: CD90=95.5%, CD105=72.6% and minimally expressed CD31=0.230% and CD45=1.42% (hematopoietic markers). The data were representative of three independent experiments, as mean \pm SD. Negative control samples were incubated with mouse IgG1-FITC/PE isotype antibodies to help differentiate nonspecific background signals from specific antibody signals.

Structural determination of TNTs and F+TNT formation

The XRD data for the sample synthesized at 120°C is consistent with the standard Anatase (USnano-America) pattern. Usually, diffraction peaks at 30°C indicate the presence of crystal defects or long-term non-sequence in TiO₂ nanoparticles. However, such a peak was not observed in our diffraction pattern which suggests the pure anatase phase of TiO₂ is formed by a quadrilateral anatase structure at 120°C. The absence of diffraction peaks at 27°C and 31°C indicates that this sample was free of rutile and TiO₂ brookite structures. The XRD pattern showed anatase phase TiO₂ nanoparticles only by diffraction at angles of 25, 37, 48, 54, 55, 63, 69, and 75°C (peak A, Fig.2A). The above results confirmed that the optimal calcination temperature for preparing pure anatase of TiO₂ nanocrystals by polymer gel was 120°C. The morphology of F+TNT formation was confirmed using SEM. It was observed that the surface area of TNT was increased compared with self-aggregation-TNT (Fig.2B).

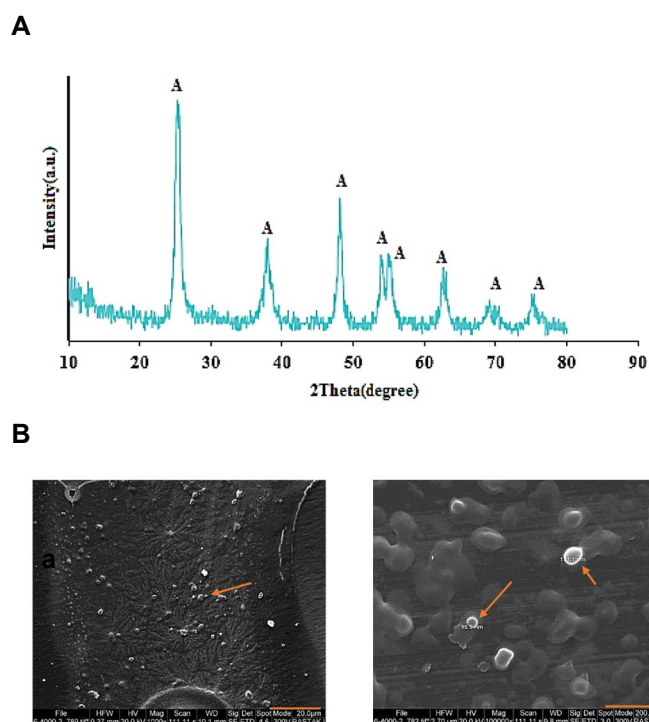


Fig.2: Structural determination of TNTs and F+TNT formation. **A.** X-ray diffraction patterns of TNT anatase phase in different angles (peak A). **B.** The SEM of F+TNT formation after 24 hours of incubation (scale bar of a: 20 µm, b: 200 nm). Orange arrows revealed the F+TNT transcription factor formation with (b) 90 to 115 nm approximate diameter. TNT; Titanium nanotube, F; Fibrin, and SEM; Scanning electron microscope.

Immunocytochemistry staining for specific oocyte-like cell marker, *MVH*, differentiation

The germ cell-related gene, *MVH*, was detected in all isolated cells using immunocytochemical analysis after 14 days. This experiment confirms that all mouse bone marrow cells have a differentiation potential into germ- and oocyte-like cells with signals and transcription factors. Under immuno-fluorescence microscopy, green fluorescent protein (*GFP*) expression was highly observed in mMSCs-derived female germ-like cells, treated with RA+F+TNT or RA compared to control cells. (Fig.3A, B).

RT-qPCR analysis of specific oocyte-like cell marker, *MVH*

RT-qPCR results show that all the cells expressed oocyte-like cell genes after 14 days of transcription factor inductions. However, the quality and quantity of expression differed among two germ cell marker groups, *MVH*. In this experiment, F+TNT transcription factors showed more significant potential to be differentiated into oocyte-like cells. A significantly higher relative gene expression level of F+TNT was observed compared with RA and control ($P < 0.05$). The results of this analysis show that co-administration of transcription factors has a higher potential for differentiation of mMSCs into female germ-like cells than individual transcription factor (Fig.4).

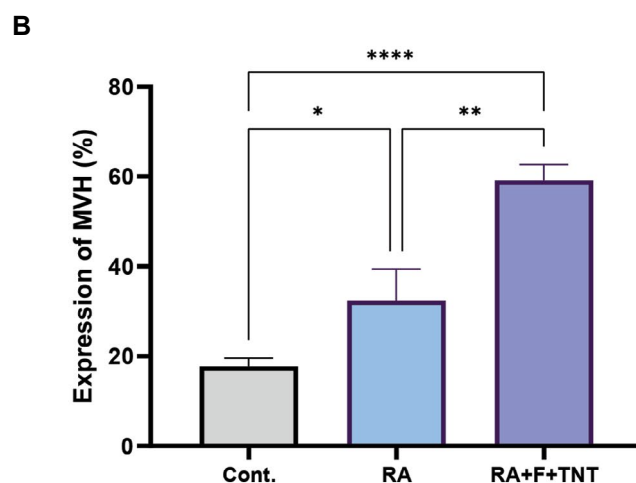
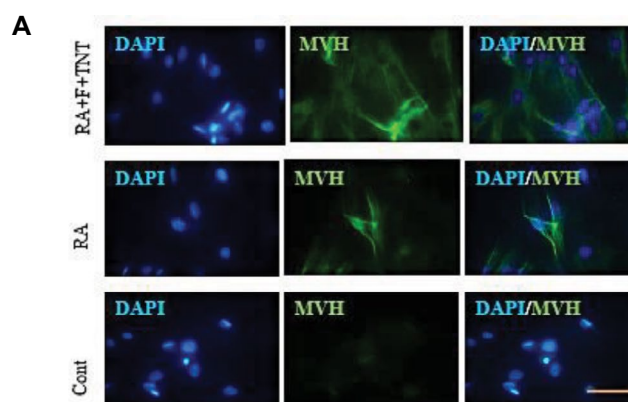


Fig.3: Expression of germ cell markers (*MVH* and *GFP*) in mMSCs-derived female germ-like cells. **A.** Immunocytochemistry staining of mMSCs for specific female germ cells marker, *MVH*, after 14 days of differentiation induction. The Nuclei were counter-stained with DAPI and GFP intensity was quantified (scale bar: 100 µm). **B.** Quantitative analysis of Immunocytochemistry images. *, $P < 0.0194$, **, $P < 0.0010$, ****, $P < 0.0001$, mMSCs; Mouse bone marrow mesenchymal stem cells, RA; Retinoic acid, F; Fibrin, Cont; Control, and TNT; Titanium nanotube.

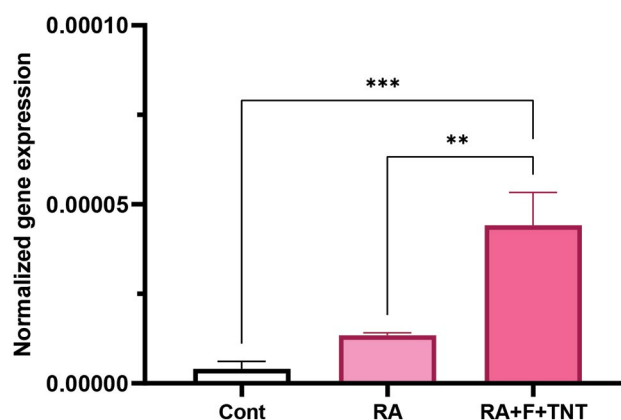


Fig.4: The RT-qPCR analysis of specific oocyte-like cell marker, *MVH*. RT-qPCR analysis of isolated mMSCs after signals and transcription factor induction under the influence of 10^{-5} M RA, 50 µg/ml TNT-coated fibrin formation for 14 days. The mMSCs treated by the RA+F+TNT compared with the RA and control cells showed significant potential to be differentiated into female germline cells due to the significantly higher relative gene expression level of *MVH* gene. **, $P < 0.0011$, ***, $P < 0.0003$, RT-qPCR; Quantitative transcription-polymerase chain reaction, mMSCs; Mouse bone marrow mesenchymal stem cells, RA; Retinoic acid, F; Fibrin, and TNT; Titanium nanotube.

Western blots of oocyte marker

Western blot analysis measured the expression of female germ cell-associated proteins (MVH) during oocyte-like cells formation from mMSCs after being cultured for 14 days. Furthermore, the level of MVH protein was higher in mMSCs treated with RA or RA+F+TNT compared to the level of MVH protein in the control cells (Fig.5).

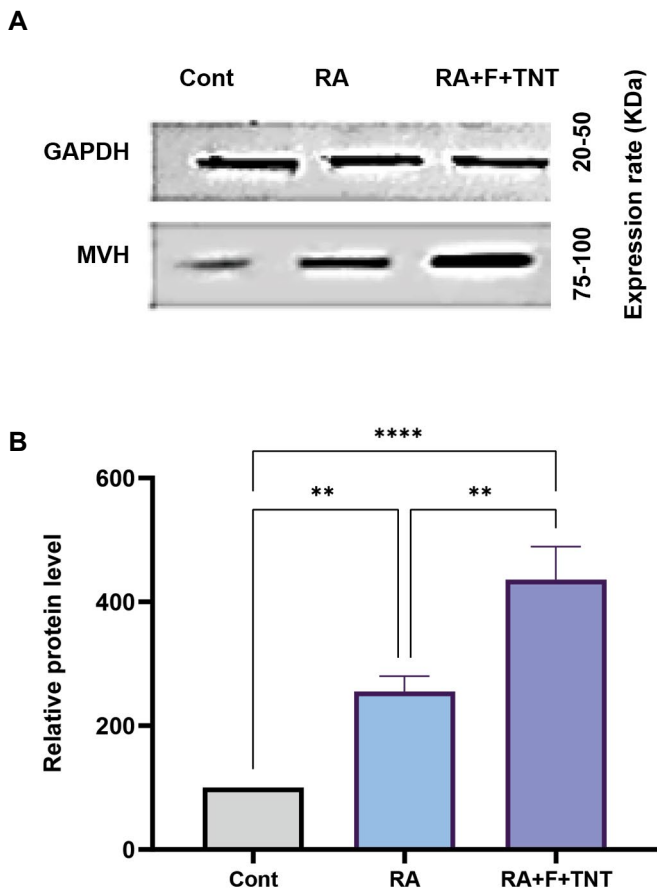


Fig.5: Western blot analysis of MVH expression in mice bone marrow-derived mMSCs. **A.** MVH protein levels were evaluated as specific differentiation markers to compare GAPDH reference protein using western blot analysis. **B.** Protein lysates from mMSCs were blotted and stained by MVH antibody. The level of MVH protein expression was higher in mMSCs treated with RA or RA+F+TNT compared to the level of MVH protein expression in the control cells. **, $P < 0.0034$, ****, $P < 0.0001$, indicated significant differences in the MVH expression between RA+F+TNT, RA, and the control, mMSCs; Mouse bone marrow mesenchymal stem cells, RA; Retinoic acid, F; Fibrin, and TNT; Titanium nanotube.

The mMSCs characterizations and signal epigenetic reprogramming for induced oocytes

The mMSCs from mice bone marrow were successfully cultured up to 4 passages, and the proliferation rate was confluency after 4-5 days following each passage. All cells had spindle-like morphology and, in some cases, possessed some long and short processes. During differentiation induction, the cells were treated with RA, RA+F+TNT formation for 14 days and observed every day to determine any differential morphological changes

under a phase-contrast microscope. In addition, size measurement and counting of oocytes were quantified using Image J software (v.1.52) (Fig.6).

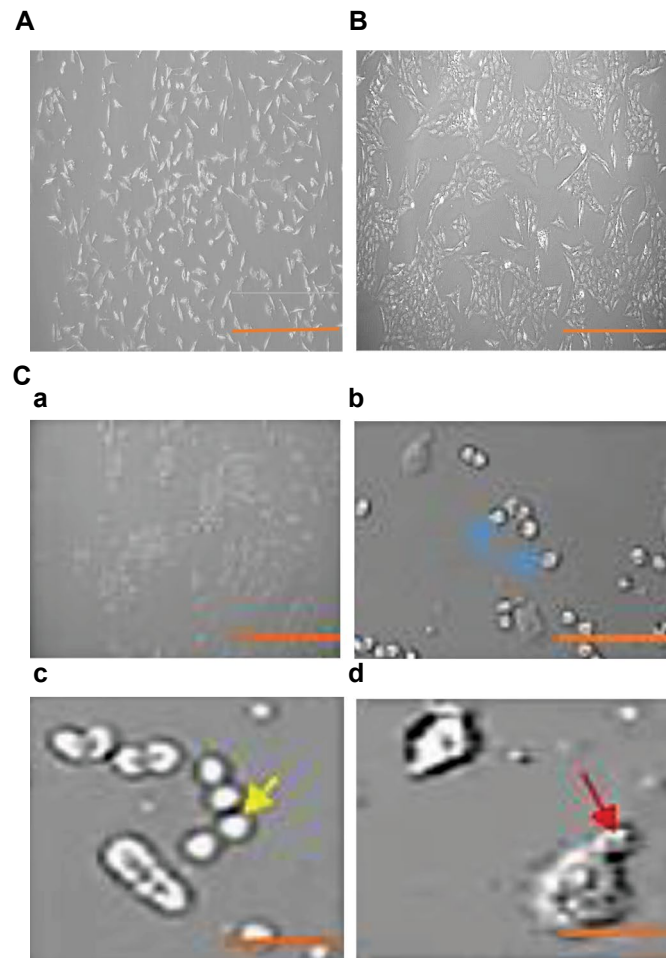


Fig.6: The isolated mMSCs and induced germ cells. **A.** Isolated mMSCs, passage 2, 24 hours after incubation (scale bar: 100 μ m). **B.** Spindle-shaped fibroblast-like of mMSCs, passage 3, in the 3rd passage (scale bar: 100 μ m). **C.** The mMSCs-derived oocyte-like cell size change and growth were observed after transcription factor inductions. The cell morphology was changed after F+TNT+RA treating. The first observation was the appearance of spindle-shaped mMSCs, which became large, circular, and long. The germ cells show a meiotic marker (MVH/DDX4). **a.** Oocyte-like cells generated from *in vitro* culturing (scale bar: 200 μ m), **b.** Primary oocyte with its nucleus arrested at prophase I of meiosis I, germinal vesical (GV), blue arrows (scale bar: 100 μ m), **c.** Primary oocyte-like cells undergoing meiosis I-nucleus and nucleolus have disappeared, germinal vesicle breakdown (GVBD), metaphase I (M I), yellow arrow, (scale bar: 50 μ m), and **d.** Secondary oocyte-like cells with the polar body (PB) resulting from meiosis I. Metaphase II (M II), red arrow (scale bar: 25 μ m).

Discussion

This study defines a set of transcription factors, which are promoted the differentiation of oocyte-like cells from mMSCs *in vitro*, which is expressed germ-like cell marker MVH/DDX4 at both mRNA and protein levels. This study will be a powerful protocol to elevate our understanding of the mechanisms underlying reprogramming in oocyte-like cell growth and of their potential application in IVF technologies.

Oocyte differentiation and development depend on continuous signaling interactions with somatic follicle cells *in vivo* (24). Signaling molecules; maturation-promoting factor (MPF), transcription, and translation of critical regulatory enzymes are the processes by which an oocyte acquires meiotic competence *in vivo*. The complex interaction between these factors and the determination of arrest versus progression is related to the delicate balance between the production and targeted degradation of signaling molecules, MPF (25-31). Finally, dysfunction on the molecular level, errors in MPF, and aberrations in chromosomal/spindle formation lead to meiotically oocyte maturation arrest. In the case of reports, changes in gonadotropin stimulation protocol, using IVM, and ICSI does not improve the treatment outcome for bad egg syndrome (3).

RA has been proven to act as a meiosis-inducing factor of meiosis in mouse gonads. RA induces *Stra8*, an RA-responsive gene in female primordial germ cell (PGCs), leading to meiosis in fetal female germ cells. Recently, reports have shown that RA can induce meiosis in PGCs before gonadal sex differentiation (32-37).

This study introduced several transcription factors, RA, RA+F+TNT, that can induce mMSCs into oocyte-like cells *in vitro*. Growth and differentiation factors can adhere to nanomaterial and fibrin, which enhance their effective delivery in culture medium and increase the developmental levels. The differentiated oocyte-like cells indicated that transcription factors are a prerequisite to activating the gene-excitatory expression driving oocyte growth *in vitro*. As such, our results complement recent studies which suggest that the principal role of epigenetic reprogramming is to activate the meiotic program. In addition, our observation showed that oocyte-like cell induction during oocyte growth is dependent on the epigenetic reprogramming in female germ-like cells. This finding provides new insight into the importance of epigenetic control and transcription factors in oocyte maturation. Furthermore, understanding possible roles of transcription factors in oocyte-like cell induction is necessary for new research. The culture conditions are a unique material that is invaluable for applications in assisted reproductive technology, such as IVM and ICSI.

Oocyte-like generation is challenging *in vitro*, and this involves both cytoplasmic and nuclear processes. This study showed the increased *MVH* expression at both mRNA and protein levels, as a result of using several transcription factors, RA, TNT, and fibrin, which indicates the effectiveness of these transcription factors in the production of female germ-like cells.

The mMSCs can be reprogrammed to an oocyte-like cell by transcription factors, RA, RA+F+TNT formation; little is known about factors that induce this reprogramming *in vivo* and *in vitro*. Furthermore, by understanding the mechanism of oocyte-like cell maturation *in vitro*, it is possible that IVM protocols could be promoted to obtain the signaling and transcription factors necessary for

oocyte maturation competence and performance *in vitro*.

Conclusion

Here, we demonstrate the induction of pluripotent stem cells from mouse bone mMSCs by introducing germ factors, *MVH*, under stem cell culture conditions and morphology determination of F+TNT induction. mMSCs exhibit the morphology and growth properties of germ-like cells and express germ cell marker genes following treatment with the above-mentioned transcription factors. These data demonstrate that oocyte-like cells can be directly generated from mMSCs by adding only a few defined factors.

Acknowledgments

We are thankful to Zohreh Mazaheri, a member of Basic Medical Sciences Research Center, Histogenotech Company, Tehran, Iran, and the laboratory assistants of the Histogenotech Company for sharing their valuable knowledge and experience in performing this study. The authors declare that there is no conflict of interests and funding support.

Authors' Contributions

S.E.; Conceived the presented idea. S.E., A.Sh., P.M., A.H.; Developed the proposal and performed the experiments. P.M., A.H.; Verified and monitored the analytical methods. S.E., A.Sh.; Investigated morphology characteristics of the TNTs and the TNTs-coated fibrin. A.Sh., P.M., A.H.; Supervised the findings of this work. All authors read and approved the final manuscript.

References

1. Bar-Ami S, Zlotkin E, Brandes JM, Itskovitz-Eldor J. Failure of meiotic competence in human oocytes. *Biol Reprod*. 1994; 50(5): 1100-1107.
2. Avrech OM, Goldman GA, Rufas O, Stein A, Amit S, Yoles I, et al. Treatment variables in relation to oocyte maturation: lessons from a clinical micromanipulation-assisted in vitro fertilization program. *J Assist Reprod Genet*. 1997; 14(6): 337-342.
3. Beall S, Brenner C, Segars J. Oocyte maturation failure: a syndrome of bad eggs. *Fertil Steril*. 2010; 94(7): 2507-2513.
4. Wang S, Wang X, Ma L, Lin X, Zhang D, Li Z, et al. Retinoic acid is sufficient for the *in vitro* induction of mouse spermatocytes. *Stem Cell Reports*. 2016; 7(1): 80-94.
5. Volarevic V, Bojic S, Nurkovic J, Volarevic A, Ljubic B, Arsenijevic N, et al. Stem cells as new agents for the treatment of infertility: current and future perspectives and challenges. *Biomed Res Int*. 2014; 2014: 507234.
6. Hübner K, Fuhrmann G, Christenson LK, Kehler J, Reinbold R, De La Fuente R, et al. Derivation of oocytes from mouse embryonic stem cells. *Science*. 2003; 300(5623): 1251-1256.
7. Bahmanpour S, Zarei Fard N, Talaei Khozani T, Hosseini A, Esmaeilpour T. Effect of BMP 4 preceded by retinoic acid and co-culturing ovarian somatic cells on differentiation of mouse embryonic stem cells into oocyte like cells. *Dev Growth Differ*. 2015; 57(5): 378-388.
8. Chimene D, Alge DL, Gaharwar AK. Two-dimensional nanomaterials for biomedical applications: emerging trends and future prospects. *Adv Mater*. 2015; 27(45): 7261-7284.
9. Solanki A, Kim JD, Lee KB. Nanotechnology for regenerative medicine: nanomaterials for stem cell imaging. *Nanomedicine (Lond)*. 2008; 3(4): 567-578.
10. Hou Y, Cai K, Li J, Chen X, Lai M, Hu Y, et al. Effects of titanium nanoparticles on adhesion, migration, proliferation, and differen-

- tiation of mesenchymal stem cells. *Int J Nanomedicine*. 2013; 8: 3619-3630.
11. Kubo K, Tsukimura N, Iwasa F, Ueno T, Saruwatari L, Aita H, et al. Cellular behavior on TiO₂ nanonodular structures in a micro-to-nanoscale hierarchy model. *Biomaterials*. 2009; 30(29): 5319-5329.
 12. Duong H, Wu B, Tawil B. Modulation of 3D fibrin matrix stiffness by intrinsic fibrinogen–thrombin compositions and by extrinsic cellular activity. *Tissue Eng Part A*. 2009; 15(7): 1865-1876.
 13. Ziv-Polat O, Skaat H, Shahar A, Margel S. Novel magnetic fibrin hydrogel scaffolds containing thrombin and growth factors conjugated iron oxide nanoparticles for tissue engineering. *Int J Nanomedicine*. 2012; 7: 1259-1274.
 14. Rampichová M, Buzgo M, Míčková A, Vocetková K, Sovková V, Lukášová V, et al. Platelet-functionalized three-dimensional poly-ε-caprolactone fibrous scaffold prepared using centrifugal spinning for delivery of growth factors. *Int J Nanomedicine*. 2017; 12: 347-361.
 15. Janmey PA, Winer JP, Weisel JW. Fibrin gels and their clinical and bioengineering applications. *J R Soc Interface*. 2009; 6(30): 1-10.
 16. De Melo BAG, Jodat YA, Cruz EM, Benincasa JC, Shin SR, Porcionatto MA. Strategies to use fibrinogen as bioink for 3D bioprinting fibrin-based soft and hard tissues. *Acta Biomater*. 2020; 117: 60-76.
 17. Khoshnood N, Zamanian A, Massoudi A. Mussel-inspired surface modification of titania nanotubes as a novel drug delivery system. *Mater Sci Eng C Mater Biol Appl*. 2017; 77: 748-754.
 18. Lopez A. Respiratory system, thoracic cavity and pleura. Pathologic basis of veterinary disease. St. Louis, Mo: Mosby Elsevier; 2007; 463-558.
 19. García-Hevia L, Valiente R, Martín-Rodríguez R, Renero-Lecuna C, González J, Rodríguez-Fernández L, et al. Nano-ZnO leads to tubulin microtubule assembly and actin bundling, triggering cytoskeletal catastrophe and cell necrosis. *Nanoscale*. 2016; 8(21): 10963-10973.
 20. Anselmo AC, Zhang M, Kumar S, Vogus DR, Menegatti S, Helgeson ME, et al. Elasticity of nanoparticles influences their blood circulation, phagocytosis, endocytosis, and targeting. *ACS Nano*. 2015; 9(3): 3169-3177.
 21. Noori A, Ashrafi SJ, Vaez-Ghaemi R, Hatamian-Zaremi A, Webster TJ. A review of fibrin and fibrin composites for bone tissue engineering. *Int J Nanomedicine*. 2017; 12: 4937-4961.
 22. Asgari HR, Akbari M, Yazdekhasti H, Rajabi Z, Navid S, Aliakbari F, et al. Comparison of human amniotic, chorionic, and umbilical cord multipotent mesenchymal stem cells regarding their capacity for differentiation toward female germ cells. *Cell Reprogram*. 2017; 19(1): 44-53.
 23. Li P, Hu H, Yang S, Tian R, Zhang Z, Zhang W, et al. Differentiation of induced pluripotent stem cells into male germ cells in vitro through embryoid body formation and retinoic acid or testosterone induction. *Biomed Res Int*. 2013; 2013: 608728.
 24. Clarke HJ. Regulation of germ cell development by intercellular signaling in the mammalian ovarian follicle. *Wiley Interdiscip Rev Dev Biol*. 2018; 7(1): 10.
 25. Jamnongjit M, Hammes SR. Oocyte maturation: the coming of age of a germ cell. *Semin Reprod Med*. 2005; 23(3): 234-241.
 26. Dekel N. Cellular, biochemical and molecular mechanisms regulating oocyte maturation. *Mol Cell Endocrinol*. 2005; 234(1-2): 19-25.
 27. Nakanishi T, Kubota H, Ishibashi N, Kumagai S, Watanabe H, Yamashita M, et al. Possible role of mouse poly (A) polymerase mGLD-2 during oocyte maturation. *Dev Biol*. 2006; 289(1): 115-126.
 28. Rauh NR, Schmidt A, Bormann J, Nigg EA, Mayer TU. Calcium triggers exit from meiosis II by targeting the APC/C inhibitor XErp1 for degradation. *Nature*. 2005; 437(7061): 1048-1052.
 29. Eichenlaub-Ritter U, Peschke M. Expression in in-vivo and in-vitro growing and maturing oocytes: focus on regulation of expression at the translational level. *Hum Reprod Update*. 2002; 8(1): 21-41.
 30. Liang CG, Su YQ, Fan HY, Schatten H, Sun QY. Mechanisms regulating oocyte meiotic resumption: roles of mitogen-activated protein kinase. *Mol Endocrinol*. 2007; 21(9): 2037-2055.
 31. Huo LJ, Fan HY, Zhong ZS, Chen DY, Schatten H, Sun QY. Ubiquitin–proteasome pathway modulates mouse oocyte meiotic maturation and fertilization via regulation of MAPK cascade and cyclin B1 degradation. *Mech Dev*. 2004; 121(10): 1275-1287.
 32. Zhou Q, Li Y, Nie R, Friel P, Mitchell D, Evanoff RM, et al. Expression of stimulated by retinoic acid gene 8 (Stra8) and maturation of murine gonocytes and spermatogonia induced by retinoic acid in vitro. *Biol Reprod*. 2008; 78(3): 537-545.
 33. Zhou Q, Nie R, Li Y, Friel P, Mitchell D, Hess RA, et al. Expression of stimulated by retinoic acid gene 8 (Stra8) in spermatogenic cells induced by retinoic acid: an in vivo study in vitamin A-sufficient postnatal murine testes. *Biol Reprod*. 2008; 79(1): 35-42.
 34. Trautmann E, Guerquin MJ, Duquenne C, Lahaye JB, Habert R, Livera G. Retinoic acid prevents germ cell mitotic arrest in mouse fetal testes. *Cell Cycle*. 2008; 7(5): 656-664.
 35. Li H, Kim KH. Retinoic acid inhibits rat XY gonad development by blocking mesonephric cell migration and decreasing the number of gonocytes. *Biol Reprod*. 2004; 70(3): 687-693.
 36. Adams IR, McLaren A. Sexually dimorphic development of mouse primordial germ cells: switching from oogenesis to spermatogenesis. *Development*. 2002; 129(5): 1155-1164.
 37. Best D, Sahlender DA, Walther N, Peden AA, Adams IR. Sdmg1 is a conserved transmembrane protein associated with germ cell sex determination and germline-soma interactions in mice. *Development*. 2008; 135(8): 1415-1425.